Optical CO Gas Sensor Using a Cobalt Oxide Thin Film Prepared by Pulsed Laser Deposition under Various Argon Pressures

Hyun-Jeong Nam, Takeshi Sasaki, and Naoto Koshizaki*

Nanoarchitectonics Research Center (NARC), National Institute of Advanced Industrial Science and Technology (AIST), Central 5, 1-1-1 Higashi, Tsukuba, Ibaraki 305-8565, Japan

Received: June 6, 2006; In Final Form: August 27, 2006

An optical CO gas sensor was investigated using cobalt oxide thin films prepared by pulsed laser deposition. The cobalt oxide films were deposited on quartz glass and silicon wafer substrates in Ar at 0.07−133 Pa. The morphology and crystal phase of the films were changed by Ar pressure. Sensitivity was estimated as the transmittance change of the film in dry air and at 200 ppm of CO gas ambient at 350 °C. The morphology of the films greatly affected the sensing properties. The optimum Ar pressure for cobalt oxide film preparation for CO gas sensing was suggested to be 13.3 Pa, based on the relationship between the morphology and the optical sensor properties of the films.

1. Introduction

Cobalt oxide is one of the more versatile oxide materials among the transition metal oxides.[1] It has been extensively investigated in view of its application as a sensor,[2] catalyst,[3,4] and magnetic material.[5,6] Recently, cobalt oxide film has attracted interest for possible application in optical gas sensors. Conventional electronic gas sensors use resistance changes to detect gas. In contrast, the optical gas sensors detect gas using optical property changes, such as transmittance or absorbance. Therefore, optical gas sensors have several advantages over electronic gas sensors; for example, they are unaffected by electromagnetic noise, they are safe in flammable gases, and they hold many possibilities over a wide range of applications.[7] Cobalt oxide film for optical gas sensors has been deposited by various methods, such as spin coating,[7,8] sputtering,[9] dip coating,[10] and pulsed laser deposition (PLD). The morphology of the cobalt oxide film is expected to be different depending upon the deposition method.

Recently, our group reported an optical CO gas sensor using cobalt oxide films prepared by PLD.[11] This optical gas sensor can detect CO gas by the transmittance change of the film with a reversible phase transition between CoO and Co_3O_4 in different ambient gases: CO and dry air. Our optical gas sensor exhibited remarkably high sensitivity because it uses the phase transition of the whole film. This is quite different from other optical gas sensors, such as NiO, Co_3O_4, and Mn_3O_4,[8,12,13] reported by other researchers that utilize a change of free electron density in the film. In conventional electronic gas sensors, sensitivity was reported to change with the morphology of film.[14,15] Also, in an optical gas sensor, the sensitivity is expected to be affected by the film morphology. However, the relationship between sensitivity and the morphology of an optical gas sensor has not yet been sufficiently investigated. PLD has high potential for producing films that have rough surfaces by controlling laser conditions.[16−18] The gas pressure of PLD is one of the important parameters controlling the film morphology.[19−21] Previously, our group investigated the effect of ambient gas for PLD on the products, and we confirmed that Ar ambient gas allows us to obtain films with nanoparticles within a certain pressure range.[22]

In this paper, we report the influence of Ar pressure for PLD on the morphology and sensing properties of the cobalt oxide films. Furthermore, the relationship between morphology and sensor properties will also be demonstrated, and the optimum Ar pressure to prepare a suitable optical gas sensor will be discussed.

2. Experimental Section

Quartz glass (for sensitivity measurement) and silicon wafer (for field emission scanning electron microscopy (FE-SEM) observation) substrates were placed in an off-axis geometry to a target in a deposition chamber. The substrate was $20 \times 10 \times 1$ mm^3; however, the cobalt oxide film was only deposited in a 10×10 mm^2 area on the substrate, using masks 5 mm wide at both ends of the substrate. A CoO single crystal was used as the target. The deposition chamber was evacuated to a base pressure of 2.66×10^{-4} Pa and then filled with Ar gas at pressures varying from 0.07 to 133 Pa. The beam of the third harmonic (355 nm) of a Q-switched Nd:YAG laser (Continuum, Precision 8000), operated at 10 Hz with 70 mJ/pulse and a pulse width of 5−7 ns, was focused on the surface of the target with a 2-mm diameter. PLD was performed for 13 min at room temperature. The substrate and target were rotated at 30 rpm during PLD.

The morphology of the films was observed using FE-SEM (Hitachi S-4800). Crystallinity comparison and phase identification were performed by X-ray diffraction (XRD, Rigaku RAD-C) using Cu Kα radiation. Film thicknesses were measured by a stylus profilometer (Kosaka, ET 4000A) at 50 μN of measuring force.

To measure the optical gas sensor properties, the prepared film was vertically mounted in a special quartz glass cell installed in a UV−vis spectrophotometer (Shimadzu UV-3100PC). The volume of the special quartz glass cell was 10 cm^3. Sensor response was measured at 350 °C by changing the gas from dry air to 200 ppm of CO balanced with nitrogen gas.

* To whom correspondence should be addressed. E-mail: koshizaki.naoto@aist.go.jp.

10.1021/jp063484f CCC: $33.50
Published on Web 10/20/2006

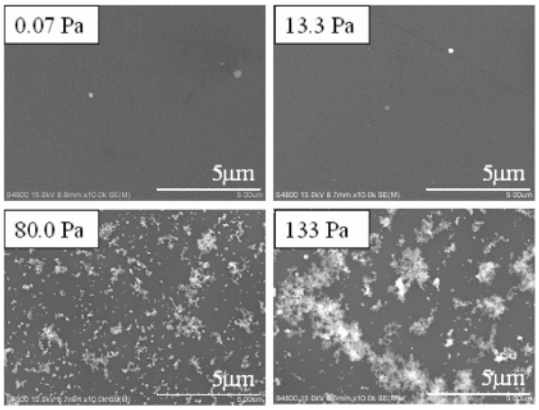

Figure 1. Low-resolution FE-SEM images of films prepared by PLD under various Ar pressures.

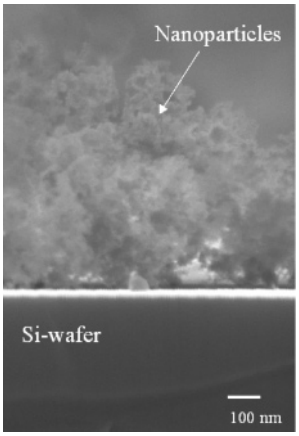

Figure 2. Cross-sectional FE-SEM image of deposits prepared at 133 Pa. Deposits consisted of nanoparticle aggregates of micrometer order size and a subjacent film with nanometer order thickness.

The gas flow rate was kept at 0.5 L/min. The optical transmittance change of the film was monitored at 625 nm.

3. Results and Discussion

3.1. Characterization of Films. Cobalt oxide films were prepared in Ar at 0.07, 0.67, 13.3, 80.0, and 133 Pa. Figure 1 presents low-resolution FE-SEM images of these films. The surface morphologies of the films differed with different Ar pressures. The films deposited at low and medium Ar pressures (0.07, 0.67, and 13.3 Pa) were smooth and adhered firmly to substrates (the film deposited in 0.67 Pa is not displayed in Figure 1). In contrast, the films prepared at high Ar pressures (80.0 and 133 Pa) consisted of two parts: nanoparticle aggregates and a thin film strongly fixed on the substrate surface (subjacent thin film) (Figures 1 and 2). Nanoparticle aggregates increased in number and density with increased Ar pressure. The nanoparticle aggregates on the film did not adhere firmly to subjacent thin films, which were easily removed even by a gentle wipe with soft paper. In contrast, the subjacent thin films were firmly fixed like those prepared at low and medium pressures.

The thicknesses of the films deposited at 0.07 and 0.67 Pa were estimated at less than 10 nm, while those deposited at 13.3 Pa were estimated at ~40 nm, based on the results from the stylus profilometer. However, the thickness of subjacent thin films deposited at high pressure was estimated to be less than 10 nm. In contrast, the thickness of the nanoparticle aggregates could not be measured, although it appears to be micrometer order in size based on the cross-sectional images by FE-SEM (Figure 2).

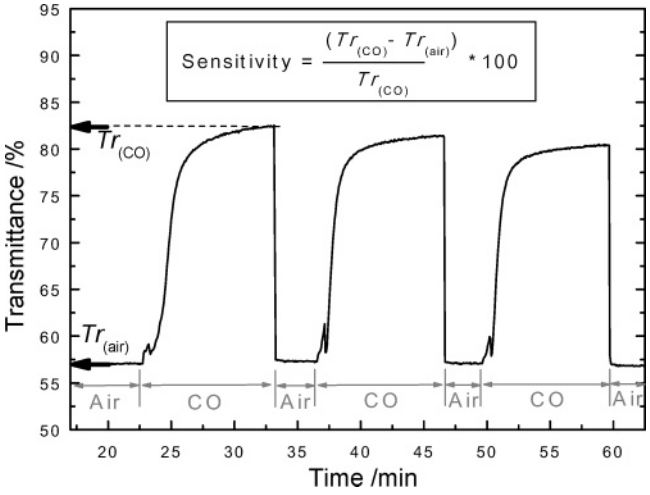

Figure 3. Transmittance change of a cobalt oxide film prepared at 133 Pa of Ar. The transmittance of the film at 625 nm was monitored in dry air and 200 ppm of CO gas at 350 °C. Sensitivity is defined as $(Tr_{(CO)} - Tr_{(air)})/Tr_{(CO)} \times 100$, where $Tr_{(CO)}$ and $Tr_{(air)}$ are transmittance in CO gas and dry air, respectively, at 350 °C.

The crystal phases of films identified by XRD also differed by Ar pressure. The films deposited at low and medium Ar pressures presented CoO peaks, whereas those deposited at high pressures exhibited a mixture phase of Co_3O_4 and CoO. In this investigation, however, we will not discuss the detailed crystal phase of the as-deposited films because the whole films were oxidized and changed to Co_3O_4 in a heating process to the sensor operating temperature of 350 °C in dry air before CO exposure.

3.2. Sensitivity of the Sensor to CO Gas. Figure 3 illustrates the transmittance change of the film prepared in Ar at 133 Pa, along with the ambient change from dry air to CO at 350 °C. We reported that the mechanism of this optical gas sensor was related to the phase transition between Co_3O_4 and CoO in our previous paper.[23] When the ambient gas was changed from dry air to CO at 350 °C, the transmittance increased by phase transition from Co_3O_4 to CoO. When the ambient gas was changed to dry air after CO exposure for 10 min, the transmittance rapidly decreased by oxidation from CoO to Co_3O_4. This reaction process was repeated four times for each film to check the sensor stability.

We compared the sensitivity of each film using a transmittance change at the initial exposure to CO gas. The sensitivity of a film is defined as follows:

$$\text{sensitivity} = \frac{(\text{Tr}_{(CO)} - \text{Tr}_{(air)})}{\text{Tr}_{(CO)}} \times 100$$

$Tr_{(CO)}$ and $Tr_{(air)}$ are transmittance in CO gas and dry air, respectively, ambient at 350 °C. The sensitivity of each film obtained at various pressures is summarized in Figure 4. The films prepared at 0.07 and 0.67 Pa exhibited low sensitivity. In contrast, the films deposited at 13.3 Pa indicated five times higher sensitivity than films deposited at 0.07 and 0.67 Pa.

As already noted in section 3.1, the three films prepared at 0.07, 0.67, and 13.3 Pa adhered firmly to substrates without nanoparticle aggregates, whereas the two films prepared at 80.0 and 133 Pa were composed of nanoparticle aggregates and subjacent films. Considering the results shown in Figure 4, along with the morphologies of the films, the nanoparticle aggregates seem to contribute to high sensitivity because both films with nanoparticle aggregates exhibited high sensitivity. To confirm this, we measured the sensitivity of the subjacent film alone,

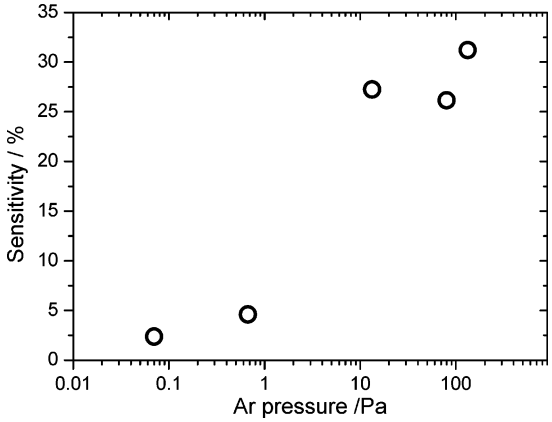

Figure 4. Sensitivity of cobalt oxide films prepared at various Ar pressures.

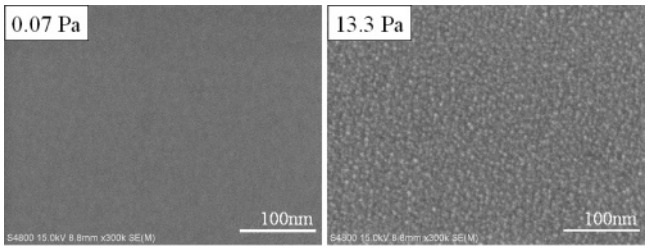

Figure 5. High-resolution FE-SEM images of films prepared by PLD at 0.07 and 13.3 Pa.

after the mechanical removal of the aggregates from the films obtained at high pressure by a wipe with soft paper. The sensitivity was greatly degraded to less than 1.5%. This result confirms that nanoparticle aggregates mostly contribute to the sensitivity of deposits prepared at high pressure.

However, the reason why only the film prepared at 13.3 Pa without nanoparticle aggregates had high sensitivity is not clear from the morphology indicated in Figure 1. Figure 5 presents high-resolution FE-SEM images of the films prepared at 0.07 and 13.3 Pa. The film deposited at 0.07 Pa had almost no structure, probably because it was very dense and the crystal size was very small. In contrast, the film deposited at 13.3 Pa appeared to have rough surfaces composed of crystallites smaller than 6 nm. The low sensitivity of the film prepared at 0.07 Pa is probably due to the high density of the film. Durrani et al. reported that a decrease in the film density increased the gas sensitivity of an electronic sensor using SnO_2.[24] Our result agrees with this report. Furthermore, the thickness of the film was also reported to affect sensitivity. Yamazaki et al. reported that the sensitivity of SnO_2 films decreased as they became less than 30 nm thick.[25] The thicknesses of our films were less than 10 and 40 nm for those deposited at 0.07 and 13.3 Pa, respectively. Thus, the high density and thinness of the film prepared at 0.07 Pa are believed to be the reason for its low sensitivity.

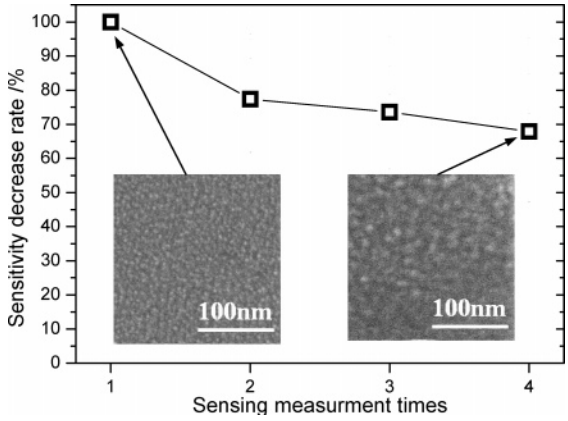

Figure 6. Relative sensitivity change obtained by iterative sensor property measurements to CO gas at 350 °C for a film prepared at 13.3 Pa. Sensitivity at the initial measurement was set as 100%. Insets are FE-SEM images of an as-deposited film prepared at 13.3 Pa and the film after a fourth exposure to CO for sensor property measurements.

3.3. Optimum Ar Pressure for the Optical Gas Sensor.

From the above results, we confirmed that Ar pressure greatly affected the morphology and sensor properties of the films. The results are summarized in Table 1. The film prepared at low Ar pressure was not suitable because it was too dense and thin to have high sensitivity. In contrast, the film prepared at high pressure was mechanically too weak to use as a gas sensor, although it presented high sensitivity. The film prepared at 13.3 Pa Ar pressure was, therefore, considered to be suitable for an optical gas sensor in terms of sensitivity and mechanical strength, and it is expected to become a promising optical gas sensor.

We measured sensitivity changes by repeated exposure to CO gas for the film prepared at 13.3 Pa. Figure 6 presents the relative CO gas sensitivity change compared to the initial sensitivity determined by iterative sensor measurement. The relative sensitivity decreased with the iterative measurement. This decrease is believed to be due to the change of film morphology by phase transformation, as shown in the FE-SEM images in Figure 6. The crystal size of the film after iterative sensor measurement more than doubled compared to that of the as-deposited film. This also revealed that the morphology of the film greatly affected the sensitivity of the optical gas sensor. Thus, the grain growth should be suppressed for multiple sensor uses.

4. Conclusions

We investigated the effect of Ar pressure during deposition on the morphology and CO gas sensing properties of cobalt oxide films deposited by PLD. The Ar pressure influenced the morphology of the films, and the morphology remarkably affected the sensor properties. The films deposited at medium

TABLE 1: Morphology and Sensor Properties of Films Deposited at Various Ar Pressures

Ar pressures / Properties	Low (0.07 and 0.67 Pa)	Medium (13.3 Pa)	High (80.0 and 133 Pa)
Schematic image	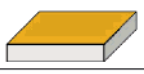	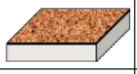	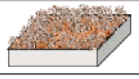
Sensitivity	Low	High	High
Mechanical stability	High	High	Low
Morphology	Smooth surface	Rough surface	Nanoparticles and rough film
Film thickness	< 10 nm	ca. 40 nm	Only subjacent film thickness < 10 nm

(13.3 Pa) and high (80.0 and 133 Pa) Ar pressures exhibited high sensitivity. However, the sensitivities of the films prepared at high pressures mostly derived from nanoparticle aggregates that attached very weakly to subjacent films. Therefore, the film prepared at the medium Ar pressure was suitable as an optical-sensing film for CO with high sensitivity and good mechanical stability.

References and Notes

(1) Patil, P. S.; Kadam, L. D.; Lokhande, C. D. *Thin Solid Films* **1996**, *272*, 29−32.

(2) Logothetis, E. M.; Park, K.; Meitzler, A. H.; Laud, K. R. *Appl. Phys. Lett.* **1975**, *26*, 209−211.

(3) Jansson, J.; Palmgvist, A. E. C.; Fridell, E.; Skoglundh, M.; Osterlund, L.; Thormahlen, P.; Langer, V. *J. Catal*. **2002**, *211*, 387−397.

(4) Thormahlen, P.; Skoglundh, M.; Fridell, E.; Andersson, B. *J. Catal.* **1999**, *188*, 300−310.

(5) Martens, J. W. D.; Peeters, W. L.; Van Noort, H. M.; Erman, M. *J. Phys. Chem. Solids* **1985**, *46*, 411−416.

(6) Miyatani, K.; Kohn, K.; Kamimura, H.; Iida, S. *J. Phys. Soc. Jpn.* **1966**, *21*, 464−468.

(7) Ando, M.; Kobayashi, T.; Haruta, M. *Catal. Today* **1997**, *36*, 135−141.

(8) Ando, M.; Kobayashi, T.; Haruta, M. *Sens. Actuators, B* **1996**, *32*, 157−160.

(9) Ko, Y. K.; Park, D. S.; Seo, B. S.; Shin, H. J.; Kim, J. Y.; Lee, J. H.; Lee, W. H.; Reucroft, P. J.; Lee, J. G. *Mater. Chem. Phys.* **2003**, *80*, 506−564.

(10) Armelao, L.; Barreca, D.; Gross, S.; Martucci, A.; Tieto, M.; Tondello, E. *J. Non-Cryst. Solids* **2001**, *293*−*295*, 477−482.

(11) Koshizaki, N.; Narazaki, A.; Sasaki, T. *Scr. Mater.* **2001**, *44*, 1925−1928.

(12) Boccuzzi, F.; Chiorino, A.; Tsubota, S.; Haruta, M. *Sens. Actuators, B* **1995**, *24*−*25*, 540−543.

(13) Martucci, A.; Pasquale, M.; Guglielmi, M.; Post, M.; Pivin, J. C. *J. Am. Ceram. Soc.* **2003**, *86*, 1638−1640.

(14) Jin, Z.; Zhou, H. J.; Jin, Z. L.; Savinell, R. F.; Liu, C. C. *Sens. Actuators, B* **1998**, *52*, 188−194.

(15) Comini, E.; Guidi, V.; Frigeri, C.; Riccò, I.; Sberveglieri, G. *Sens. Actuators, B* **2001**, *77*, 16−21.

(16) Sánchez Aké, C.; Sobral, H.; Villagrán Muniz, M.; Escobar-Alarcón, L.; Camps, E. *Opt. Lasers Eng.* **2003**, *39*, 581−588.

(17) Szörényi, T.; Geretovszky, Zs. *Thin Solid Films* **2004**, *453*−*454*, 431−435.

(18) Chrisey, D. B.; Hubler, G. K. *Pulsed Laser Deposition*; Wiley: New York, 1994.

(19) Zeng, X.; Koshizaki, N.; Sasaki, T. *Appl. Phys. A: Mater. Sci. Process.* **1999**, *69*, S253−S255.

(20) Syarif, D. G.; Miyashita, A.; Yamaki, T.; Sumita, T.; Choi, Y.-S.; Itoh, H. *Appl. Surf. Sci.* **2002**, *193*, 287−292.

(21) Afonso, C. N.; Gonzalo, J.; Serna, R.; de Sande, J. C. G.; Ricolleau, C.; Grigis, C.; Gandais, M.; Hole, D. E.; Townsend, P. D. *Appl. Phys. A: Mater. Sci. Process*. **1999**, *69*, S201−S207.

(22) Zbroniec, L.; Sasaki, T.; Koshizaki, N. *Appl. Phys. A: Mater. Sci. Process.* **2004**, *79*, 1783−1787.

(23) Nam, H. J.; Sasaki, T.; Koshizaki, N. In *Nanoparticles and Nanostructures in Sensors and Catalysis*, Materials Research Society Symposium Proceedings, Warrendale, PA, 2005; Zhong, C.-J., Kotov, N. A., Daniell, W., Zamborini, F. P., Eds.; 0900-O09-17.

(24) Durrani, S. M. A.; Khawaja, E. E.; Al-kuhaili, M. F. *Talanta* **2005**, *65*, 1162−1167.

(25) Yamazaki, T.; Okumura, H.; Jin, C. J.; Nakayama, A.; Kikuta, T.; Nakatani, N. *Vacuum* **2005**, *77*, 237−243.